Journal of Ceramic Processing Research. Vol. 24, No. 4, pp. 634~639 (2023)
(Received 18 March 2023, Received in revised form 17 June 2023, Accepted 6 July 2023)
https://doi.org/10.36410/jcpr.2023.24.4.634

J O U R N A L O F
Ceramic Processing Research

Influence of $ZnFe_2O_4$ substitution on the microstructural and magnetic properties of M-type $Sr_{0.1}Ca_{0.4}La_{0.5}Fe_{12}O_{19}$ hexagonal ferrites

Xiubin Zhao and Ailin Xia*
School of Materials Science and Engineering, Anhui University of Technology, Maanshan 243002, China

The M-type ferrite $Sr_{0.1}Ca_{0.4}La_{0.5}Fe_{12}O_{19}$ magnetic powders with different $ZnFe_2O_4$ substitution amounts (R_m, 0, 1%, 3%, 5%, 7%, and 9%) were obtained using a ceramic process. The structure of specimens were examined by using an X-ray diffractometer. All the specimens exhibited a typical single-phase hexagonal M-type structure, and the particles in specimens were uniformly distributed in size. The VSM study indicated the specimen with R_m=9% had the maximum saturation magnetization of 70.22 emu/g, and the residual magnetization and the coercivity of specimens increased firstly and decreased later with the increase of R_m. The specimen with R_m=3% exhibits the best comprehensive magnetic properties.

Keywords: Ferrite, $ZnFe_2O_4$ substitution, Ceramic method, Magnetic properties.

Introduction

Hexagonal M-type $AFe_{12}O_{19}$ (A=Sr, Ba and Pb) ferrite is one of the most widely used hard magnetic materials mainly due to its fine corrosion resistance, low cost and good chemical stability [1-7]. In order to improve the magnetic properties of M-type hexaferrites, adding or doping some elements is widely studied. The substitution of rare earths and transition metals such as La^{3+}, Ce^{3+}, Ni^{2+}, Ti^{4+}, Co^{2+}, Mn^{2+}, Cu^{2+}, Mg^{2+}, and Zn^{2+} on Fe^{3+} have been investigated extensively as well as some co-substitutions, such as Co-Ti, La-Co, La-Cu and La-Zn [8-17]. The M-type hexaferrites with high magnetic properties are mainly the La-Co substituted $BaFe_{12}O_{19}$ (BaM) and $SrFe_{12}O_{19}$ (SrM) ferrites. In order to reduce the cost of M-type hexaferrites, Zn^{2+} ions were used to replace Co^{2+} ions because the cost of ZnO powder is much cheaper than that of CoO powder. L.S. You et al. [18] prepared SrM ferrite substituted by La-Zn via a self-propagating high-temperature synthesis method, and it was found that the La-Zn substitution significantly improved the magnetic properties of M-type strontium ferrite. Vinnik et al. [19] prepared the Zn-substituted $BaZn_xFe_{12-x}O_{19}$ ($0 < x < 0.065$) single crystals and found that the saturation magnetization (M_s) and coercivity (H_c) depended very sensitively on the amount of Zn-substitution. Asghar et al. [20] synthesized Cr-Zn-doped SrM nanoparticles $SrFe_{12-2x}$-$Cr_xZn_xO_{19}$ (x=0.0-0.8) by chemical coprecipitation method and found that both M_s and H_c decreased with the increasing Cr-Zn content, and the dielectric constants, together with the dielectric losses, decreased with the increase of doping content. Xia et al. [2] have synthesized $Ba(Zn\ Ti)_xFe_{12-2x}O_{19}$ (x = 0.0, 0.2, 0.6, 1.0, 1.4) M-type Ba ferrite powders via a new route by combining a chemical coprecipitation technique and found that small quantities of ZnTi substitutions helps to form single-phase ferrite at a low calcination temperature, the magnetic properties were reduced obviously with the increase of x from 0.2 to 1.4. M.J. Iqbal et al. [21] have prepared the Zr-Zn substituted M type strontium ferrite nanoparticles by a chemical coprecipitation method. The results show that the M_s, magnetic moment and remanent magnetism (B_r) increased with the increase of the amount of substitution, but coercivity decreases with the increase of the amount of substitution.

In our previous study, the performance of ferrite can be significantly improved by the exchange coupling between soft and hard magnetic phases. Up to the present, the effects of pure $ZnFe_2O_4$ substitution on the microstructural and magnetic properties of the SrCaLa hexaferrites obtained via a ceramic process was still not reported. In this study, influence of $ZnFe_2O_4$ additive on the microstructural and magnetic properties of M-type $Sr_{0.1}Ca_{0.4}La_{0.5}Fe_{12}O_{19}$ hexagonal ferrites was studied, which may help to reduce the use of rare earth elements in high-performance SrM ferrites.

Experimental Procedures

Synthesis of $ZnFe_2O_4$ powders

A ceramic process was used to obtain $ZnFe_2O_4$ (ZFO) powders. Analytically pure Fe_2O_3 and ZnO were used as raw materials without further treatment. The

*Corresponding author:
Tel : +86 13665557919
Fax: +86 05552311570
E-mail: alxia@126.com

mixed powders (Fe_2O_3 and ZnO) were ball-milled in water for 2 h with an angular velocity of 400 rpm and a ball-to-powder weight ratio of 15:1. The as-milled powders were dried, sifted and then calcined in a muffle at 850 °C for 3 h in an air atmosphere. Finally, the calcined samples were pulverized to powders with a size of smaller than 100 μm using a vibration mill.

Preparation of M-type ferrite $Sr_{0.1}Ca_{0.4}La_{0.5}Fe_{12}O_{19}$ (SrCaLaM)powders with ZFO additive

All samples of $Sr_{0.1}Ca_{0.4}La_{0.5}Fe_{12}O_{19}$ powders with different amount of ZFO (R_m, 0%, 1%, 3%, 5%, 7% and 9%) were obtained using a ceramic process. The starting materials used were $SrCO_3$ (98% purity), $CaCO_3$ (99% purity), La_2O_3 (99% purity), and Fe_2O_3 (98% purity). The mixed powders were milled in water for 2 h with an angular velocity of 400 rpm and a ball-to-powder weight ratio of 15:1, together with ZFO of different R_m. The obtained powders were dried, sifted and then sintered at 1300 °C for 2 h in a muffle furnace with an air atmosphere. Finally, the sintered specimens were pulverized to powders with a size of smaller than 100 μm using a vibration mill.

Characterization

The phase composition of the materials was decided by a powder X-ray diffractometer (XRD, Rigaku D/max-2550V/PC) using Cu K_α (λ=1.5406Å) radiation. The 2θ angles were scanned over a range between 10° and 80°. A field emission scanning electron microscope (FESEM, HITACHI S-4800) was utilized to analyze the morphology. The room temperature (RT) magnetic hysteresis loops of samples were measured on a vibrating sample magnetometer (VSM, MicroSense EZ7) with a maximum external field of 1592 kA/m (20000 Oe).

Results and Discussion

Phase Identification and microstructure

Fig. 1 gives the XRD patterns of the as-synthesized SrCaLaM (R_m=0%) and ZFO powders. The only diffraction peaks from SrCaLaM (R_m=0%) (pdf no 33-1340) and ZFO (pdf no 22-1012) can be found in Fig. 1(a) and (b), respectively, indicating the single-phase structure of specimens.

Fig. 2 shows the XRD patterns of the hexaferrite SrCaLaM magnetic powders with different R_m ranging from 1% to 9%. Compared with the standard XRD pattern of strontium ferrite (JCPDS card no. 22-1340), only typical peaks from single-phase magnetoplumbite SrCaLaM was found, which implies that the Zn^{2+} ions entered into the magnetoplumbite lattice without producing any second phase.

The lattice constants a and c can be calculated using the values of Miller indices (h, k, l) and the inter-planer spacing d_{hkl} corresponding to (107) and (114) peaks

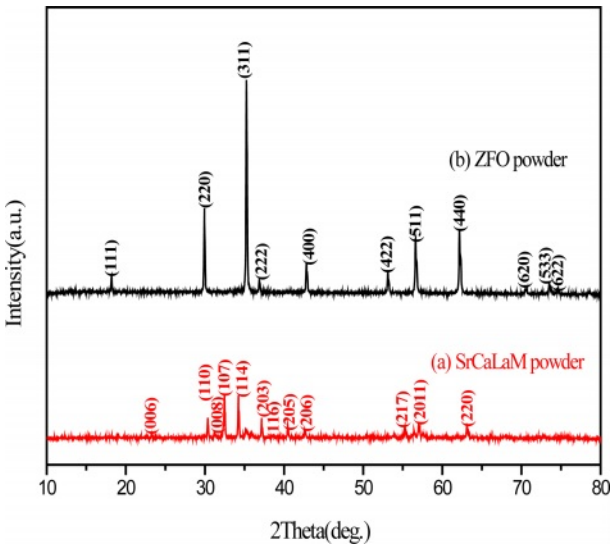

Fig. 1. XRD patterns of as-synthesized SrCaLaM (R_m=0%) and ZFO powders.

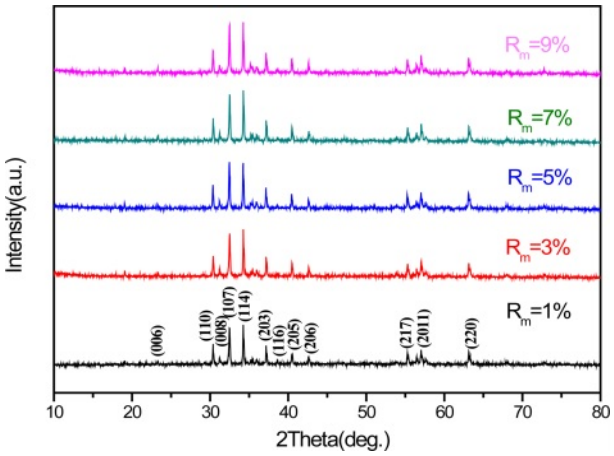

Fig. 2. XRD patterns of the hexaferrite SrCaLaM magnetic powders with different R_m.

according to the following formula (1):

$$d_{hkl} = \left(\frac{4}{3} \cdot \frac{h^2 + hk + k^2}{a^2} + \frac{l^2}{c^2} \right)^{-1/2} \quad (1)$$

Fig. 3 indicates the change in crystal axis ratio of c/a in different samples. As shown in this figure, the c/a changed slightly with the increase of R_m. According to Verstegen and Stevels [22], the ratio of c/a may present the structure type of Sr ferrites. For the M-type structure, the c/a was assumed to be smaller than 3.98. Herein, the values of c/a range from 3.8960 to 3.9006, which seems to be in well accord with the reported values of M-type structure.

Tipical FESEM images of samples are presented in Fig. 4. It can be observed that the all the samples consist of relatively uniform particles with typical hexagonal structure. It can be found that compared with the sample with R_m=0%, the average particle size

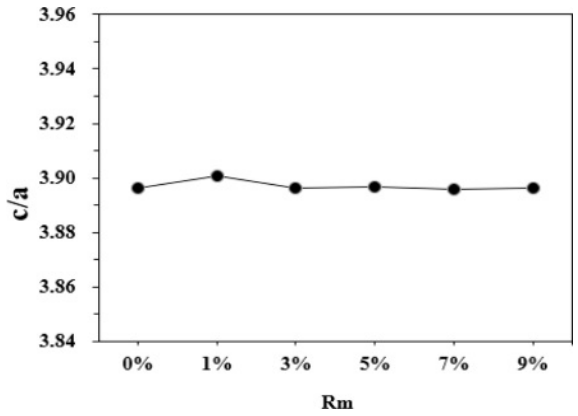

Fig. 3. The crystal axis ratio of c/a of the hexaferrite SrCaLaM magnetic powders with different R_m.

of samples with ZFO addictiveis obviously smaller. The addition of ZFO plays the role of refining grain and preventing grain growth. However, with the increase of R_m, the typical morphology and the average particle size of specimens did not change obviously.

Magnetic properties

The room-temperature magnetic hysteresis loops of samples with R_m are shown in Fig. 5, and the corresponding M_s, H_c and M_r of samples are listed in Table 1. What should be pointed out is that since the magnetic hysteresis loops were roughly saturated at a field of 1592 kA/m (20000 Oe), the value of magnetization obtained at 1592 kA/m (20000 Oe) is approximately used as M_s.

As can be seen from Table 1 and Fig. 6, it appears

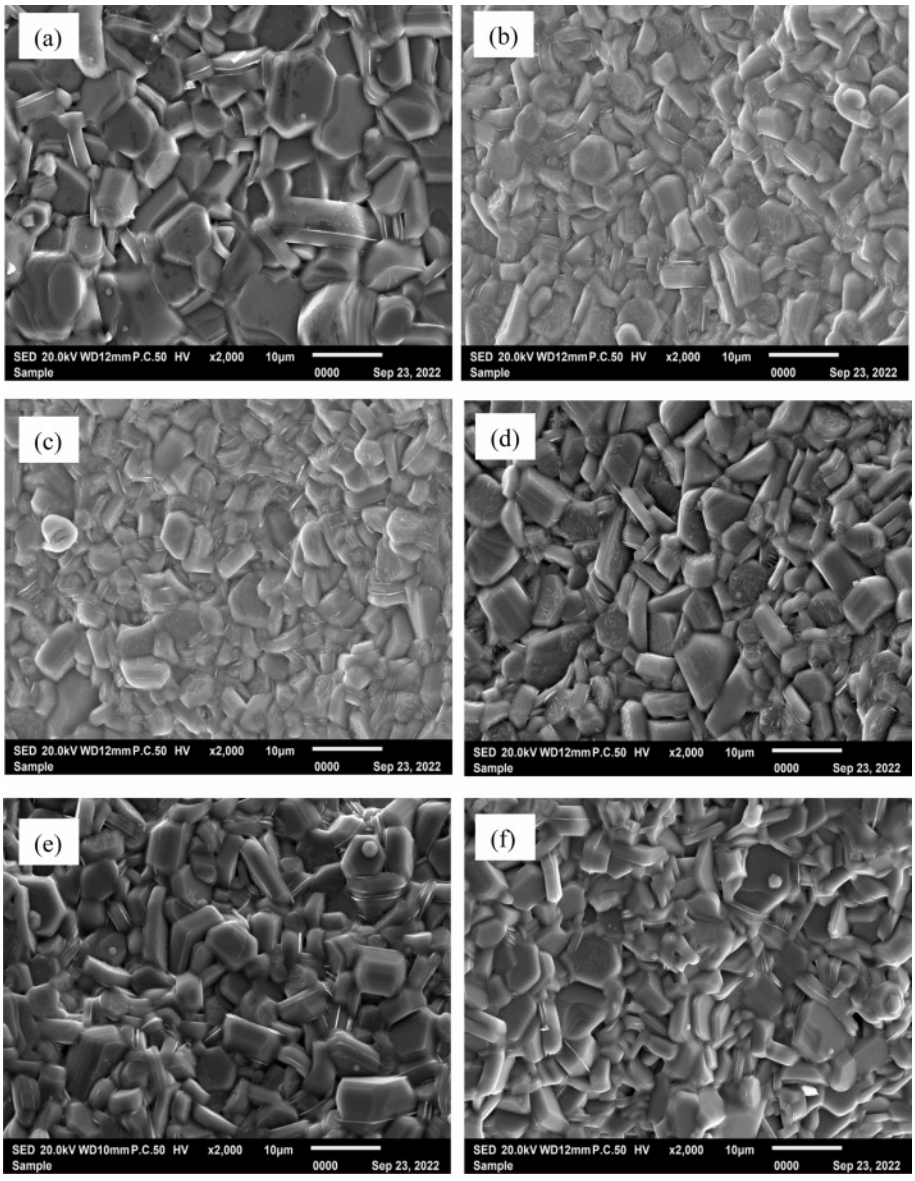

Fig. 4. Typical SEM images of the hexaferrite SrCaLaM magnetic powders with different R_m.: (a) 0%, (b) 1%, (c) 3%, (d) 5%, (e) 7% and (f) 9%.

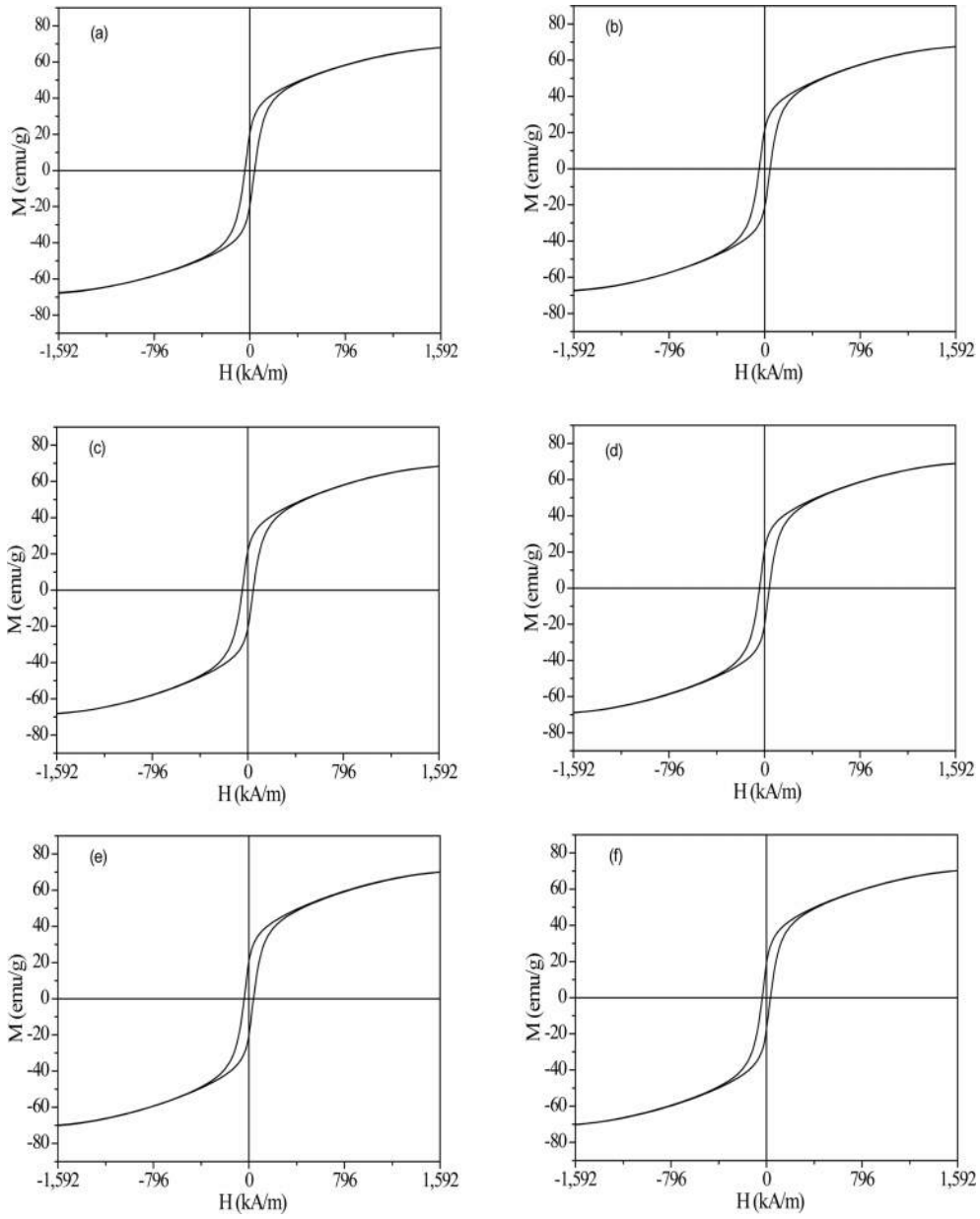

Fig. 5. RT magnetic hysteresis loops of specimens with different R_m. R_m: (a) 0%, (b) 1%, (c) 3%, (d) 5%, (e) 7%, and (f) 9%.

Table 1. Magnetic properties of samples with different R_m.

ZFO substitution (R_m)	M_s (emu/g)	M_r (emu/g)	H_c (kA/m)
0%	67.32	19.92	40.45
1%	67.45	21.36	45.35
3%	68.24	21.29	45.54
5%	68.96	20.77	40.78
7%	70.09	20.45	38.94
9%	70.22	17.98	34.34

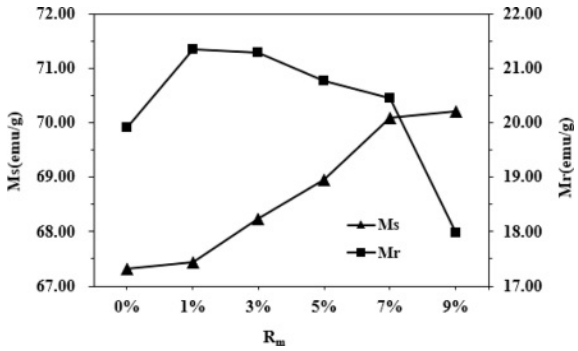

Fig. 6. The M_s and M_r of samples with different R_m.

that the variation of M_s and M_r is obvious for different R_m. The M_s of samples increases with the increase of R_m from 0% to 9%, and it reaches 70.22 emu/g when R_m=9%. The M_r of specimens increases with the increase of R_m from 0% to 1%, while it decreases when

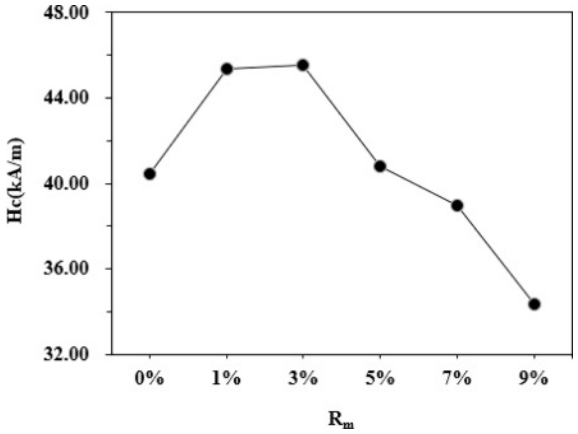

Fig. 7. The H_c of samples with different R_m.

R_m increases from 1% to 9%. The maximum M_r is 21.36 emu/g (R_m=1%). The effects of different R_m on the H_c of samples have been presented in Fig. 7 and Table 1. It is apparent that the H_c of samples first increases from 40.45 kA/m (508 Oe) (at R_m=0%) to 45.54 kA/m (572 Oe) (at R_m=3%), which is the maximum value of H_c. However, with a further increase of R_m from 3% to 9%, the H_c decreases continuously to 34.34 kA/m (431 Oe) at R_m=9%. The sample with R_m=3% exhibits the relatively good magnetic properties, among which the M_s is 68.24 emu/g, the M_r is 21.29 emu/g and the H_c is 45.54 kA/m (572 Oe).

In the M-type hexaferrite crystal structure, Fe^{3+} ions occupy five different sites, including the spin up sites 2a, 2b and 12k as well as the spin down sites $4f_1$ and $4f_2$. S.W. Lee et al. [23] and L. Lechevallier et al. [24] reported that Zn^{2+} ions preferentially replace Fe^{3+} ions at $4f_1$ spin-down sites, which will result in an increase of the number of spin-up Fe^{3+} ions compared with that of spin-down Fe^{3+} ions. J.M. Bai et al. [25] reported that for a large amount of La-Zn substitution, the substitution of Fe^{3+} ions by Zn^{2+} ions can lead to the weakening of the strength of superexchange, which will lead to the transformation of the colinear arrangement of Fe^{3+} ions to the non-colinear arrangement, accompanied by the spin-inclined structure. Therefore, as the R_m increases from 0% to 1%, the occupation of Zn^{2+} at $4f_1$ sites reduces the spin down magnetic moment and enhances the overall magnetic moment, and correspondingly the M_r increases. It is well-known for the M-type hexaferrites that the magnetic moments of Fe^{3+} ions are arranged collinearly due to existence of superexchange interaction [26]. The decrease of M_r with R_m from 1% to 9% are due to the weakening of Fe^{3+}-O-Fe^{3+} superexchange interaction strength at the 12k- and 2b-sites. It was found that the H_c of specimens increases first and then decreases with the increase of R_m. It is commonly known that the H_c is mainly dependent on the magnetic crystal anisotropy. Therefore, the increasing H_c for R_m from 0% to 3% can be attributed to the increasing magnetocrystalline anisotropy field after the introduction of ZFO substitution. However, since Zn^{2+} is a kind of non-magnetic ion, the substitution of magnetic ion Fe^{3+} will inevitably reduce the total magnetic crystal anisotropy constant and the anisotropy field, thereby leading to the decrease of H_c. J.C. Corral-Huacuz et al. [27] and X.Q. Shen et al. [28] reported that the decrease of H_c with the increasing Zn^{2+} ion amount was mainly due to the decrease of magnetic crystal anisotropy constant caused by the substitution of Fe^{3+} ions with Zn^{2+} ions.

Conclusions

The M-type ferrite $Sr_{0.1}Ca_{0.4}La_{0.5}Fe_{12}O_{19}$ ferrite powders with different ZFO substitution amount (R_m, 0%, 1%, 3%, 5%, 7% and 9%) were obtained using a ceramic process. The XRD patterns showed that the single magnetoplumbite phase was obtained in the magnetic powders with the increasing R_m from 0% to 9%. The SEM study manifested that the particles were distributed uniformly in the samples. The VSM study indicated the magnetic properties were affected by the R_m greatly due to the occupation sites of Zn^{2+}. It was found that the sample with R_m=3% exhibits the relatively good magnetic properties of M_s=68.24 emu/g, M_r=21.29 emu/g and H_c=45.54 kA/m (572 Oe). According to this study, the SrM ferrites can be manufactured more economically through adding the low-cost ZFO to reduce the usage of rare earth elements.

References

1. S. Zhang, C.X. Cao, S.B. Su, A.L. Xia, H.Y. Zhang, H.L. Li, Z.Y. Liu, and C.G. Jin, J. Adv. Ceram. 12[4] (2023) 815-821.
2. A.L. Xia, D.X. Du, P.P. Li, and Y.X. Sun, J. Mater. Sci: Mater Electron 22 (2011) 223-227.
3. M.M. Hessien, M.M. Rashad, M.S. Hassan, and K. El-Barawy, J. Alloy. Compd. 476 (2009) 373-378.
4. A.L. Xia, C.H. Zuo, L. Chen, C.G. Jin, and Y.H. Lv, J. Magn. Magn. Mater. 332 (2013) 186-191.
5. L. Qiao, B. Xu, Q. Xi, J. Zheng, and L. Jiang, Ceram. Int. 36 (2010) 1423-1427.
6. D.T.M. Hue, P. Lampen, T.V. Manh, and V.D. Viet, J. Appl. Phys. 114 (2013) 1191.
7. F.Y. Wang, J.J. Ji, C.X. Cao, C.Z. Gong, A.L. Xia, H.Y. Zhang, H.L. Li, Z.Y. Liu, and C.G. Jin, J. Phys. Chem. Sol. 163 (2022) 110565.
8. X. Liu, W. Zhong, S. Yang, Z. Yu, B. Gu, and Y. Du, J. Magn. Magn. Mater. 238 (2002) 207-214.
9. X.B. Zhao, S. Zhang, J.S. Li, A.L. Xia, and Y.J. Yang, J. Ceram. Process. Res. 24 (2023) 98-102.
10. Y. Yang, X. Liu, D. Jin, and Y. Ma, Mater. Res. Bull. 59 (2014) 37-41.
11. Y.J. Yang, F.H. Wang, X.S. Liu, J.X. Shao, and D.H. Huang, J. Magn. Magn. Mater. 421 (2017) 349-354.
12. C.J. Li, B. Wang, and J.N. Wang, J. Magn. Magn. Mater. 324 (2012) 1305-1311.
13. B.K. Rai, S.R. Mishra, and V.V. Nguyen, J. Alloys

Compd. 550 (2013) 198-203.
14. Y.J. Yang, F.H. Wang, J.X. Shao, M.L. Li, and D.H. Huang, J. Ceram. Process. Res. 18 (2017) 151-155.
15. P.A.M. Castellanos, A.C.M. Borges, G.O. Melgar, J.A. Garcia, and E.G. Alcaide, Physica B 406 (2011) 3130-3136.
16. W. Zhang, B. Yang, H. Xi, L. Wang, X. Lu, and L. Qiao, J. Alloys Compd. 546 (2013) 234-238.
17. Y.J. Yang, F.H. Wang, J.X. Shao, and Q.L. Cao, J. Ceram. Process. Res. 17 (2016) 615-619.
18. L. You, Q. Liang, J. Zheng, M. Jiang, L. Jiang, and J. Sheng, J. Rare Earth. 26 (2008) 81-84.
19. D.A. Vinnik, A.S. Semisalova, L.S. Mashkovtseva, A.K. Yakushechkina, S. Nemrava, S.A. Gudkova, D.A Zherebtsov, N.S. Perov, L.I. Isaenko, and R. Niewa, Mater. Chem. Phys. 163 (2015) 416-420.
20. P.F.S. Pereira, A.P.D. Moura, I.C. Nogueira, M.V.S. Lima, E. Longo, P.C.D.S. Filho, O.A. Serra, E.J. Nassar, and I.L.V. Rosa, J. Alloys Compd. 526 (2012) 11-21.
21. M.J. Iqbal, M.N. Ashiq, and P.H. Gomez, J. Alloys Compd. 478 (2009) 736-740.
22. G.B. Teh, Y.C. Wong, and R.D. Tilley, J. Magn. Magn. Mater. 323 (2011) 2318-2322.
23. S.W. Lee, S.Y. An, I.B. Shim, and C.S. Kim, J. Magn. Magn. Mater. 231 (2005) 290-291.
24. L. Lechevallier, J.M. Le. Breton, J.F. Wang, and I.R. Harris, J. Phys: Condens. Matter. 16 (2004) 5359-5376.
25. J.M. Bai, X.X. Liu, T. Xie, F. Wei, and Z. Yang, Mater. Sci. Eng. B 68 (2000) 182-185.
26. Y.J. Yang, F.H. Wang, J.X. Shao, X.S. Liu, S.J. Feng, and J.S. Yang, J. Magn. Magn. Mater. 401 (2016) 1039-1045.
27. J.C. Corral-Huacuz, and G. Mendoza-Suarez, J. Magn. Magn. Mater. 245 (2002) 430-433.
28. X.Q. Shen, M.Q. Liu, F.S. Song, and Y.W. Zhu, Appl. Phys. A 104 (2011) 109-116.